Microchemical Journal 199 (2024) 110093

Contents lists available at ScienceDirect

Microchemical Journal

journal homepage: www.elsevier.com/locate/microc

# Real-time characterization and quantification of aerosol components for open- and Closed-Ended heated tobacco products

Yue Zhang [a], Shaoxin Ye [b], Zuoying Wen [b], Lili Fu [a], Tao Wang [c], Ke Zhang [a,*], Chuan Liu [a], Shuang Wang [a], Xiaofeng Tang [b,*], Di Kang [c], Bing Wang [a], Bin Li [a,*]

[a] Zhengzhou Tobacco Research Institute of CNTC, Zhengzhou 450001, China
[b] Anhui Institute of Optics and Fine Mechanics, HFIPS, Chinese Academy of Sciences, Hefei 230031, China
[c] China Tobacco Hebei Industrial Co., Ltd, Shijiazhuang 050000, China

ARTICLE INFO

*Keywords:*
HTPs
Aerosol
Gas/particulate Distribution
On-line Analysis
VUV photoionization Mass spectrometry
Quantification

ABSTRACT

To characterize fast and dynamic thermophysical processes of aerosol formation from heated tobacco products (HTPs), a real-time chemical detection and quantification at sub-second time resolution is of great significance. Herein a novel vacuum ultraviolet (VUV) photoionization time-of-flight mass spectrometer (PI-TOFMS) was adapted for on-line chemical analysis of gaseous and particulate aerosol fractions formed from two HTP systems of contrasting designs. The two HTP systems used a battery-powered heating mechanism to heat tobacco rods containing granulated tobacco materials, one puffing air to flow through the tobacco bed and the other with no puffing air going through the tobacco section (termed as open-ended and close-ended, respectively). The on-line PIMS analyzer was able to detect a great number of mass peaks, including nicotine (Nic), glycerin (VG) and propylene glycol (PG) *etc* in the particulate phase, and flavor components such as 2,3-Butanedione and triethyl citrate in both gaseous and particulate phases. In particular, some short-lived intermediates such as ethenol and propen-2-ol from pyrolysis of the tobacco granules were observed and identified on-line. Nic, VG and PG were quantified with a high time resolution of 0.5 s using their standard calibration curves established with PI-TOFMS. The time-resolved evolving mass profiles of Nic, VG and PG were obtained in near real-time, as well as Nic release rate within a single puff for the first time. In addition, the present results clearly revealed that the change in puffing air flow pathway along the tobacco rod from the open-ended to the close-ended configurations significantly altered the Nic delivery pattern, in which a stable Nic delivery profile in the open-ended HTP at prolonged puff durations was reduced in the close-ended HTP. These findings can be utilized to develop suitable HTPs that could mimic the Nic delivery and hence help smokers to quit smoking.

## 1. Introduction

Cigarette smoke is a complex and fast dynamic aerosol system that consists of thousands of chemicals in both particulate and gaseous phases [1,2]. Among them, over a hundred have been recognized as hazardous and toxic substances including tobacco-specific nitrosamines, polycyclic aromatic hydrocarbons, and some volatile aldehydes [3–5]. Chronical exposure of these substances through smoking is thought to cause adverse health effects like chronic obstructive pulmonary disease (COPD), heart diseases, stroke and lung cancers. Various efforts have been made to reduce these adverse health effects from cigarette consuming, and one recent approach is to transfer the use of nicotine from tobacco combustion into tobacco heating, in which the combustion by-products of harmful nature could be reduced. This type of tobacco products is known as “heated tobacco products”, or HTPs [6,7].

Characterizing the nature of chemicals and their quantities in cigarette smoke is indispensable to reduce potential negative effects, and is very helpful to evaluate the effectiveness in any product design modification aimed at harm reduction [8–10]. Conventionally, chemical analysis of complex aerosol system is performed with particle filters, impingers or adsorption tubes followed by off-line analytical methods such as gas chromatography (GC), gas chromatography-mass spectrometry (GC–MS), liquid chromatography-mass spectrometry (LC-MS) and two-dimensional gas chromatography–time-of-flight mass spectrometry (GC × GC-TOF-MS) etc [11–14]. For example, Salman et al. [15] used high-performance liquid chromatography (HPLC) and GC

* Corresponding authors.
*E-mail addresses:* hfzhangke@126.com (K. Zhang), tangxf@aiofm.ac.cn (X. Tang), ztrilibin@163.com (B. Li).

https://doi.org/10.1016/j.microc.2024.110093
Received 11 December 2023; Received in revised form 30 January 2024; Accepted 1 February 2024
Available online 5 February 2024

system to analyze nicotine and carbonyls in HTPs smoke; Dusautoir et al. [16] used HPLC system and a multi-wavelength fluorescence detector to analyze polycyclic aromatic hydrocarbons and carbonyls in HTPs smoke; Cancelada et al. [17] used GC–MS system to detect volatile emissions from HTPs; Li et al. [10] used a GC × GC-TOF-MS to analyze volatile organic carbons in HTPs smoke. Aforementioned analytical methods provide qualitative and quantitative information on chemical species of the off-line samples. However, the passive trapping of target compounds means to preserve dynamic information or mechanisms difficult [18], especially to get the aerosol dynamics within a puff.

Aerosols from HTPs contain more liquid and semi-volatile droplets as well as much less stable carbonaceous particles compared with combustion cigarettes due to their lower working temperature, making them even more challenging to be characterized by off-line methods [19]. The time-of-flight mass spectrometry (TOF-MS) as one kind of on-line method has the advantage of high time resolution in particular combined with a soft ionization strategy (e.g. photoionization) to generate molecular ions [20], and has been used for on-line smoke analysis [21,22].

Photoionization (PI) TOF-MS have been used in characterizing gaseous components in cigarette smoke and other combustion systems. For example, Hawke et al. [23] used a soft-photon ionization (SPI) TOF-MS and standard gases to establish quantification of seven toxicants in the gas phase of cigarette mainstream smoke. Heide et al. [24] used SPI-TOF-MS to evaluate the puff-resolved gas emissions in E-cigarettes, HTPs and conventional cigarettes. Hu et al. [25] used synchrotron radiation photoionization-MS and discovered diamine, 2H-azirine, and sulfur monoxide in the gas phase of cigarette smoke. However, online qualification and quantification of the particle compositions in cigarette smoke without pretreatment is still challenging. Here we present the results of an on-line analysis of both gaseous and particulate aerosol chemicals from two HTPs heating tobacco granules using a home-made PI-TOF-MS system [26]. The two HTP systems used a battery-powered heating mechanism to heat tobacco rods containing granulated tobacco materials, one puffing air to flow through the tobacco bed (termed as open-ended) and the other with no puffing air going through the tobacco section (termed as close-ended). The combination of the design features in HTPs are novel and their aerosol release behavior was characterized on-line. The three main particulate phase components including nicotine (Nic), glycerin (VG) and propylene glycol (PG) were clearly observed within a single puff under the open-ended and close-ended air flow patterns. The on-line puff-by-puff emission signals of Nic, VG and PG were also compared to puff-by-puff mass obtained from off-line gas chromatography-thermal conductivity detector (GC-TCD) analysis based on their standard curves of quantification. In addition, effects of puff duration on chemical release were also measured, providing unparalleled insights into the aerosol formation mechanism in the HTPs.

## 2. Methods

### 2.1. HTP design and puffing regimes

The HTPs tested in this work are mainly composed of two parts: a battery-powered electronic heater and a specially formulated tobacco stick, with a total length of 45 mm and a diameter of 7.2 mm. It can be segmented into four distinct sections: a tobacco granule section (with a 15 mm length), a fixture section designed to prevent granule movement (6 mm length), a hollow tube (14 mm length) and a filter plug (10 mm length), as shown in Fig S1. The tobacco granules were made with milled tobacco powder, in which additional tobacco extract were added together with 4.7 % glycerol and 9.4 % propylene glycol. The granulation was formed by extrusion granulation process.

Two different airflow pathways in the tested HTPs were compared during the experiments as shown in Fig. 1, and these airflow pathways used different thermophysics mechanisms to extract aerosols, in which

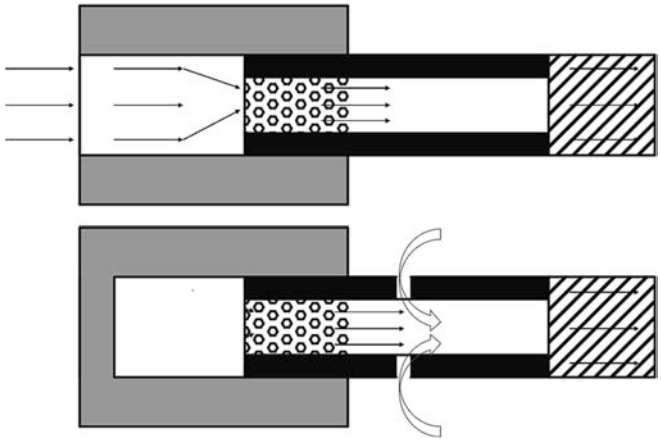

**Fig. 1.** Schematic diagram of the air flow pathways in the open-ended (up) and the close-ended (low) HTPs.

the details of the airflow mechanisms can be found in a previous work [7]. Briefly, the close-ended pathway prevented the incoming air being puffed through the tobacco granule section, maintaining a near oxygen-free environment during the course of the aerosol generation. Eight small holes for air vent were punched peripherally at the downstream airflow and the upper edge of the tobacco granule section to facilitate aerosol extraction via negative pressure generated through puffing. In contrast, no air vent holes were punched for the open-ended pathway, the puffing airflow entered from the upstream end of the tobacco granule section and traversed the entire rod.

The two airflow pathways were enacted to work with the heating devices, which used electrically resistive heating to heat the tobacco rod from the inside with the maximum heating temperature at 240℃ ± 5℃. Linear smoking machines (i-MAC600A, Zhengzhou Jiade Technology Co., Ltd) were used in both on-line and off-line experiments for aerosol generation under the Health Canada Intense (HCI) puffing regime, with a 55 mL puff volume, 2 s puff duration and 30 s puff interval. In the GC-TCD off-line tests, particles were collected on Cambridge filter pads before subsequent chemical analyses. In addition, aerosols were also generated with different puffing durations (4, 6, 8 and 10 s) by the same linear smoking machine with the same puff volume and puff intervals. For both the close-ended and open-ended HTPs, the heating period for one tobacco stick lasted for 210 s, which allowed for 8 smoking puffs under the HCI mode.

### 2.2. PI-TOF-MS analysis

A home-made PI-TOF-MS analyzer was employed for on-line analysis of both gaseous and particulate phase substances in the HTP aerosol (Fig S2). The detailed configuration of the PI-TOF-MS for the on-line aerosol sampling can be found in our previous study [26] and only a brief description is presented here. During each test, fresh aerosol stream was directly transferred into the PI-TOF-MS via a capillary inlet or an aerodynamic lens (ADL). The capillary inlet was used for gaseous or volatile substance analysis, with Cambridge filters installed in the smoking machine to remove the condense phase particles. The capillary inlet had 4 cm in length and 0.1 mm in diameter, which sampled the gaseous fraction with a flow of 4 $cm^3$/min into the photoionization zone to be ionized. For particulate phase analysis, the ADL (combination of a series of lenses and spacers) was used to sample the aerosol directly with a flow of 85 $cm^3$/min and focused the condense phase particles into the TOF-MS with no filters post aerosol generation. The accompanied gases and volatiles during the particulate analysis were removed by differential pumping of the TOF-MS. Once the aerosol particles were in the photoionization zone, they were evaporated into volatile molecules on the hot surface of a thermal desorption unit and then ionized with a

commercial krypton discharge lamp (hv = 10.6 eV, Heraeus, Hanau, Germany). A reflectron TOF mass analyzer with a mass resolving power of 2500 was employed to analyze mass of ions.

### 2.3. GC-TCD and GC–MS analysis

Nic, VG and PG are three main aerosol formers contained in the tobacco granules of the HTP sticks. They were released during heating and formed the main body of the aerosol before being deposited on Cambridge filter pads. To quantify their levels, the Cambridge filter pads were solvent extracted and then analyzed by GC-TCD [27]. The whole filter pad from a puff was extracted with 25 mL methanol while being oscillated for 90 min. One micro liter of the filter extract was injected into a GC-TCD system (GC8890, Agilent Technology, Santa Clara, CA, USA). The target analytes were separated by an HP-INNOWAX column (30 m length, 0.32 mm diameter and 0.25 mm film thickness, Agilent Technology, Santa Clara, CA, USA). The GC's oven temperatures were programmed as follows: held at 80 ℃ for 3 min, ramped to 250 ℃ with a speed of 50 ℃/min and then held for 5 min.

The main chemical components in the tobacco granules were also analyzed by GC–MS. For this purpose, tobacco granules were collected and homogenized from several cigarettes and extracted with 25 mL methanol in oscillating for 180 min before being analyzed by GC–MS. The solvent was then filtered to avoid undissolved particles. One microliter of the extract was injected into a GC–MS (GC8890/MS5977B, Agilent Technology, Santa Clara, CA, USA). The GC injector temperature was 300 ℃ and operated at splitless mode. Helium was used as carrier gas with a constant flow of 1.2 mL/min. Separation of the target analytes was conducted using a DB-5MS column (60 m length, 250 μm diameter and 1 μm film thickness, Agilent Technology). Oven temperatures for GC were programmed as follows: held at initial temperature 35℃ for 5 min, ramped to 200℃ with a speed of 2℃/min, and then ramped to 290℃ at 5℃/min and held for 15 min. The transfer line temperature was set at 300℃. Electron-impact ionization with 70 eV electron energy and source temperature of 230 ℃ was used for analysis. Target compounds were scanned and detected at a full scan mode, and the corresponding

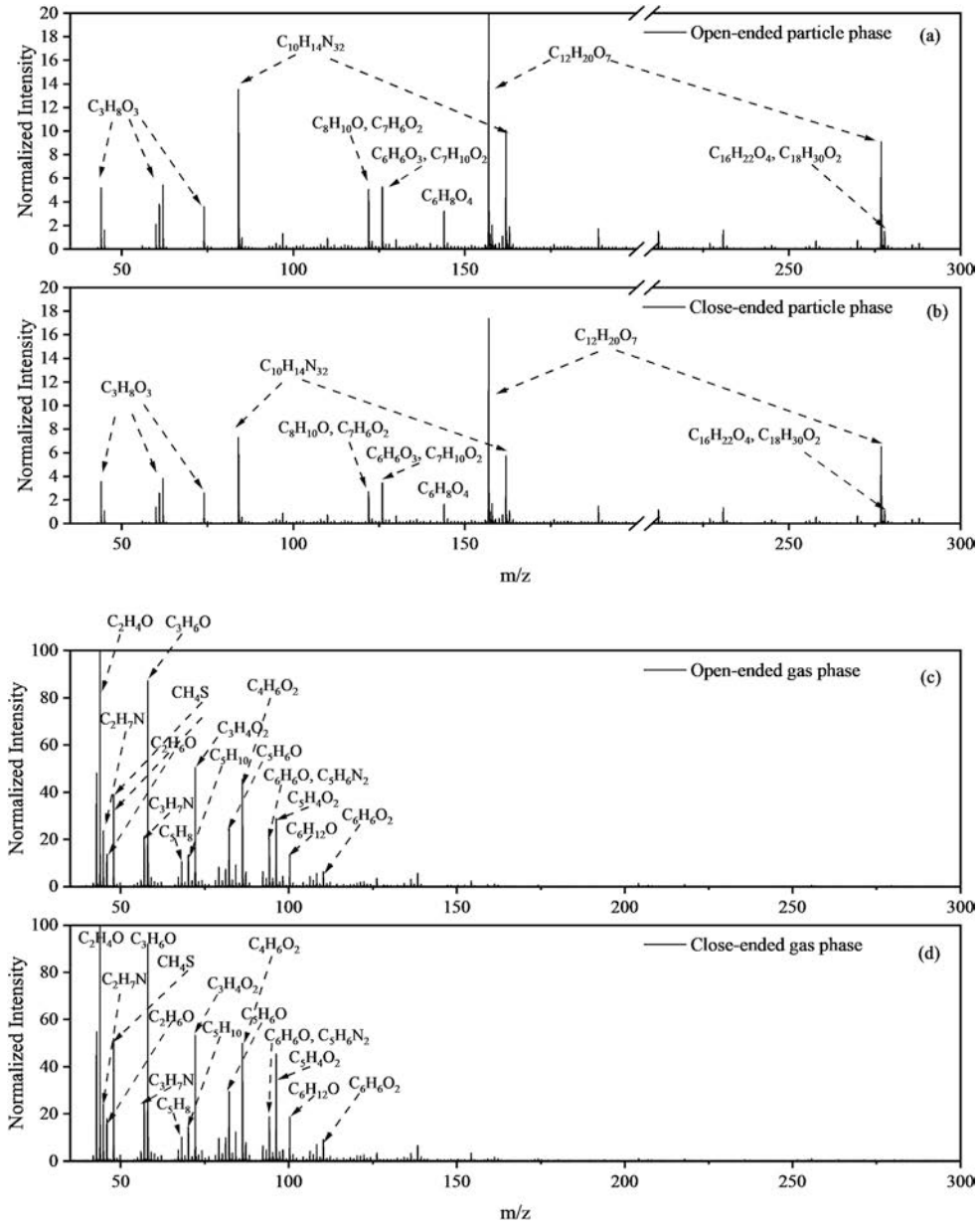


**Fig. 2.** Mass spectra of the particulate phase (a, b) and gas phase (c, d) aerosol for the open-ended and close-ended HTPs under HCI puffing mode. Intensities were normalized for particulate and gas phase, respectively.

spectrum was identified with the help of NIST.20 library for peak identification.

### 2.4. On-line quantification of Nic, VG and PG

Nic, VG and PG, the three key aerosol constituents of the HTPs, were chosen for online quantification. The strong correlation between the PI-TOF-MS signal intensity and the mass concentration prompted simultaneous online and offline tests to compare the mass (mg) and the signal intensity for the three components in puffs of varying durations (2, 4, 6 and 8 s). Puff duration of 10 s was excluded in the off-line tests due to the sub-detection-limit nicotine concentrations of off-line method. Diverse concentrations and signal intensities from the different puff durations (2, 4, 6 and 8 s) were used to establish the linear regression model.

### 2.5. Sample and data treatments

Prior to the experiments, tobacco sticks were conditioned at 22 ± 2 ℃for 48 h [7]. The heating devices were fully charged before each test, and cleaned and cooled after each test. Puff volumes were calibrated to 55 mL with a soap-film flowmeter. For both on-line and off-line tests, triplicate measurements were performed under each test condition and the results presented in average +/- standard deviations (std).

## 3. Results and discussion

### 3.1. Mass spectra of aerosol from open-ended and close-ended HTPs

Mass spectra from the open-ended and close-ended HTPs with 2 s aerosol generation are shown in Fig. 2 (average of puffs 1 to 8). Ratio of total signal intensity in gas phase and particulate phase was generally about 0.01 in 2 s aerosol generation in this study, indicating that the particulate fraction dominated in the HTPs aerosol. The gas/particle mass ratio is similar to the results conducted by off-line methods, where total particulate matter mass (without water) is more than 100 times of volatile organic compounds mass [10]. Due to the domination of particulate fractions, only particulate phase tests were conducted in puff durations of 4, 6, 8, 10 s (Fig S3). In general, various peaks were observed in the mass spectra of both open-ended and close-ended HTPs at different puff durations (Fig. 2, Fig S3). There were no significant differences for the mass peaks identified among the tests, which implied that the changes in puff durations or airflow pathways did not alter the aerosol chemical species.

The major peaks in the particulate phase could be assigned in the spectra. For common components like VG, PG and Nic, assignments were done according to their characteristic $m/z$ values under VUV-ionization condition reported in literatures [26], where VG at $m/z$ = 44, 60, 61, 62, 74, 92, PG at $m/z$ = 45, 76, Nic at $m/z$ = 84, 162 were taken. However, some components have not been studied and reported before in VUV-ionization studies. Therefore, GC–MS analysis was conducted to obtain components species and relatively ratios of the tobacco granules as shown in Table S2. Results in Table S2 were used to help the assignment of components. For example, triethyl citrate is a component detected in tobacco granules, and its characteristic $m/z$ values of 157, 203, 276 at electron ionization condition can also be observed in the VUV-PI-TOF-MS spectra. Therefore, $m/z$ values at 157, 203, 276 were assigned as triethyl citrate. According to the above methods, all peaks with a signal intensity ratio higher than 0.1 % were assigned and listed in Table1, S1.

Both VG and PG were widely used as the main aerosol formers in the tobacco reconstituted materials for HTPs, and have been identified as the main particulate phase components under the ambient condition [7]. As the heating temperature was sufficiently high to release nicotine, Nic was also one of the major aerosol components in the two HTPs. These results are similar to previously published results on HTPs where VG, PG and Nic also dominated the mass spectral responses [26]. The peaks of triethyl citrate were also observed here. As shown in Fig. 2, the mass responses of the open-ended HTP were higher than those of the close-ended HTP under the same puff duration. In addition, with increasing puff durations, for both the open-ended and close-ended HTPs the peaks of mass responses showed a decreasing trend (Fig2, S3). Despite the changes in puff durations, heating temperature and puff intervals remained stable, therefore, same amount of aerosol former were released between two puffs in those tests as a result. Longer puff durations lowered the puff flow velocity at a constant puff volume (55 mL), and therefore lowered the peaks of mass responses.

Mass spectra of the gaseous phase were also shown in Fig. 2, which was assigned follow the same method as described before. In comparison to the responses from the particulate phase aerosol, more major components were identified in the gaseous phase peak assigning, including peaks at $m/z$ = 44 (ethenol, acetaldehyde, ethylene oxide), $m/z$ = 58 (propen-2-ol, acetone, propanal), $m/z$ = 72 (acrylic acid, 2-butanone, isobutyraldehyde), $m/z$ = 86 (2,3-Butanedione) and $m/z$ = 96 (3-Furaldehyde, 4-Cyclopentene-1,3-dione). Among them, ethenol and propen-2-ol, the short-lived intermediates during ring opening reactions of VG and PG pyrolysis [25,28,29], were clearly detected here because of the sensitivity and in-situ nature of the on-line PI-TOF-MS method, both of which were lost during the sample enrichment and pretreatment processes in the previous off-line analysis. Acetaldehyde, acetone and 2-butanone were previously reported in both fresh smoke and human exhaled smoke in lit cigarettes [30]. Ethylene oxide and propanal were also detected using soft ionization mass spectrometry in smoke of a Virginia type cigarette [25]. Acrylic acid has been reported as the dehydration and oxidation product of glycerin, while isobutyraldehyde is a common component in cigarette smoke [31,32]. The components at $m/z$ = 44, 58 and 72 were not found in the granule analysis by GC–MS, implied that initial pyrolysis reactions which lead to the formation of these low-molecular weight volatile components also occurred in the aerosol generation of the HTPs. While 2,3-butanedione, an added flavoring chemical, could be observed in the mass spectra at $m/z$ = 86 [33], 3-furaldehyde, 4-cyclopentene-1,3-dione and other common substances in tobacco leaves at $m/z$ = 96 [34] were all found here in the aerosol of the granulated tobacco material, indicated that they were delivered into the aerosol by thermal distillation.

There were 35 peaks detected in the particulate phase (shown in Table 1) and 48 peaks in the gaseous phase (shown in Table S1) were identified in this study. Some peaks were found in both the open-ended and close-ended HTPs, yet their relative ratios were somewhat different for the two airflow systems. Taking PG as an example, PG ratio was lower in the particulate phase yet higher in the gaseous phase for the close-ended HTP compared to that in the open-ended HTP, implied that the close-ended airflow pathway had a lower condensation/nucleation rate than open-ended pathway. It can be proved by the ratios between the gaseous and particulate signal intensities, where the gas/particle partitioning ratios were higher in the close-ended HTP (1.18 %) than those of the open-ended HTP (0.90 %). The ambient air passing through the tobacco rod in the open-ended HTP may have led to a lower heating temperature [7], thus a higher condensation/nucleation rate was found in the close-ended HTP. These difference in the gaseous and particulate ratios were also found for some oxygenated species like aldehydes and ketones. Lower ratios at $m/z$ = 44, 58, 72 in the close-ended HTP implied that less formations of aldehydes and ketones were achieved in this airflow due to lower oxygen content as the incoming air was bypassed through the filter ventilation holes [35]. The application of the PI-TOF-MS in the aerosol analysis by separating the gaseous and particulate phase components thus did help in understanding the aerosol formation mechanisms in these two HTP configurations.

### 3.2. Variations of PG, VG, Nic signals with puff durations

The total signal intensities of PG, VG, Nic at different puff durations from the close-ended and open-ended HTPs were shown in Fig. 3 (and

**Table 1**
The major compositions of the smoke with relative ratios larger than 0.1% (in particle-phase) measured with the PI-TOF-MS.

| *m/z* | Formula | Proportion in total signal (%) | | Species | references |
|---|---|---|---|---|---|
| | | Open-ended | Close-ended | | |
| 44 | $C_3H_8O_3$ | 0.75 | 0.63 | Glycerin | [26] |
| 45 | $C_3H_8O_2$ | 0.24 | 0.19 | Propylene Glycol | |
| 60 | $C_3H_8O_3$ | 0.31 | 0.25 | Glycerin | |
| 61 | $C_3H_8O_3$ | 0.60 | 0.50 | Glycerin | |
| 62 | $C_3H_8O_3$ | 0.84 | 0.70 | Glycerin | |
| 74 | $C_3H_8O_3$ | 0.59 | 0.50 | Glycerin | |
| 76 | $C_3H_8O_2$ | 0.03 | 0.02 | Propylene Glycol | |
| 84 | $C_{10}H_{14}N_2$ | 2.48 | 1.61 | Fragmentation of Nicotine | [39] |
| 85 | $C_4H_7NO$ | 0.20 | 0.13 | Methylpyrrolidine, piperidine | [40] |
| 92 | $C_3H_8O_3$ | 0.02 | 0.02 | Glycerin | [26] |
| 95 | $C_5H_5NO$ | 0.11 | 0.10 | 3-pyridinol | |
| 96 | $C_5H_4O_2$ | 0.09 | 0.09 | 3-Furaldehyde, 4-Cyclopentene-1,3-dione | This study |
| 108 | $C_6H_8N_2$ | 0.10 | 0.11 | 2,6-Dimethylpyrazine | [26] |
| 110 | $C_6H_6O_2$ | 0.19 | 0.18 | 5-Methyl furfural, Catechol, Hydroquinone | This study |
| 122 | $C_8H_{10}O$, $C_7H_6O_2$ | 0.94 | 0.62 | Benzoic acid | |
| 123 | $C_6H_5NO_2$ | 0.17 | 0.14 | Niacin | |
| 126 | $C_6H_6O_3$, $C_7H_{10}O_2$ | 0.97 | 0.80 | Maltol, 6-Ethyl-5,6-dihydro-2H-pyran-2-one | |
| 128 | $C_6H_8O_3$, $C_7H_{12}O_2$, $C_4H_4N_2O_3$ | 0.10 | 0.09 | Furaneol, Furandimethanol | |
| 130 | $C_7H_{14}O_2$ | 0.16 | 0.16 | methylindene | [18] |
| 136 | $C_{10}H_{16}$, $C_8H_8O_2$ | 0.16 | 0.16 | Benzoic acid, methyl ester, Benzeneacetic acid, 4-Vinylbenzene-1,2-diol | This study |
| 144 | $C_6H_8O_4$ | 0.61 | 0.37 | 2,4-Dihydroxy-2,5-dimethyl-3(2H)-furan-3-one, 4H-Pyran-4-one, 2,3-dihydro-3,5-dihydroxy-6-methyl- | |
| 152 | $C_9H_{12}O_2$, $C_{10}H_{16}O$ | 0.11 | 0.11 | 4-Ethylguaiacol, 2-methyl-5-(prop-1-en-2-yl)-2-vinyltetrahydrofuran | [26] |
| 156 | $C_{10}H_8N_2$ | 0.24 | 0.24 | 2,3′-Dipyridyl | This study |
| 157 | $C_{12}H_{20}O_7$ | 5.77 | 5.93 | Fragmentation of Triethyl citrate | [41] |
| 158 | $C_{10}H_{10}N_2$ | 0.60 | 0.60 | Nicotyrine | This study |
| 162 | $C_{10}H_{14}N_2$ | 2.13 | 1.44 | Nicotine | [41] |
| 176 | $C_7H_{12}O_5$, $C_{10}H_{12}N_2O$ | 0.11 | 0.12 | 1,3-Diacetin, Cotinine | [26] |
| 203 | $C_{12}H_{20}O_7$ | 38.60 | 42.99 | Fragmentation of Triethyl citrate | [41] |
| 204 | $C_{12}H_{16}N_2O$, $C_{14}H_{20}O$, $C_{15}H_{24}$ | 3.79 | 3.62 | N-Cyclohexylnicotinamide, n-acetylanabasine, a-amylcinnamyl alcohol, *trans*-caryophyllene | [26] |
| 206 | $C_{14}H_{22}O$ | 1.75 | 1.53 | 2,4-Di-*tert*-butylphenol | This study |
| 270 | $C_{17}H_{34}O_2$, $C_{20}H_{30}$ | 0.18 | 0.19 | Methyl Hexadecanoate | |
| 276 | $C_{12}H_{20}O_7$ | 2.24 | 1.93 | Triethyl citrate | |
| 278 | $C_{16}H_{22}O_4$, $C_{18}H_{30}O_2$ | 0.39 | 0.34 | Dibutyl phthalate | |
| 288 | $C_{20}H_{32}O$ | 0.11 | 0.12 | 13,14-Dihydroretinol | [26] |

I declare on behalf of all co-authors that we have no conflicts of interest to this work. We declare that we do not have any commercial or associative interest that represents a conflict of interest in connection with the work submitted.

Fig S4), to exemplify how the puffing flow rates alter the aerosol delivery pattern. The results showed that the prolonged puff durations lowered the Nic and PG, VG deliveries in the close-ended HTP with an approximately linear trend, while no obvious variation was observed for the open-ended HTP. Due to the high sensitivity and in-situ detection of the PI-TOF-MS system, the low concentrations of Nic, PG, VG at the 10 s puff duration in the close-ended HTP could also be observed. For this HTP, prolonged puff durations lowered the flow velocity at the ventilation holes with an equal puff volume. According to the Bernoulli's law, a slower flow velocity would lead to higher pressure at the upstream thus less pressure differences between the heated granule section and the side holes, which then lowered the aerosol extraction efficiency and lead the reduction of Nic, PG, VG at the outlet. For the open-ended HTP, its aerosol was delivered by the incoming airflow that passed through the whole of tobacco bed, where a prolonged puff duration would reduce flow velocity and not change the efficiency of aerosol out of the tobacco rod with a stable puff volume.

### 3.3. *Puff-by-puff resolved aerosol mass signals and quantification of PG, VG, Nic*

Aerosol mass signals were also resolved puff-by-puff and utilized to compare the effects of the two different airflow pathways on the three main aerosol chemicals in particulate phase (Fig. 4). Generally, the puff-by-puff signal intensities of PG, VG and Nic followed an increase-first-then-decrease trend irrespective of the two airflow configurations, with the highest mass intensity obtained at the puff 5–6 for the open-ended HTP and at the puff 7 for the close-ended HTP. These release profiles are different to that of combustible cigarettes, where a steady increase in the smoke yield for most of chemicals were observed with puff number [18]. For combustible cigarettes, gradual reduction in the cigarette rod length resulted in less smoke filtration and dilution air from the cigarette wrapping paper, leading to a steady increase in the smoke yield. As shown in Fig. 4, with the changes of the puff duration, similar profiles for the three main species were observed for the open-ended HTP. On the contrary, the prolonged puff durations had a significant effect on lowering PG, VG and Nic in the close-ended HTP, in agreement with the results in Fig. 3.

Despite the high sensitivity and in-situ setup of the PI-TOF-MS system, quantification of aerosol compositions still remained difficult. Typically, internal standards with a range of concentrations and gradients were employed to establish the standard curve. Besides, internal standards need to be generated as aerosols and purged into the inlet of PI-TOF-MS to produce the response gradients for the target signal. Here, chemical concentration gradients were achieved by different puffs during smoking. Puffs 3–7 in close-ended tests and puffs 2–5 in open-ended tests give a consecutive gradient in PG, VG, Nic intensities and masses. In addition, signal intensities from the open-ended HTP were puff-by-puff accumulated to obtain higher gradients than the single puff results to cover the wide range in chemical mass (Table S3). Moreover, regressions between the puff-by-puff off-line mass values captured by Cambridge filters and the on-line signal intensities of VG, PG, Nic recorded by the PI-TOF-MS system were established (Fig. 5). As shown in Fig. 5, the coefficient of determination ($R^2$) of the regression lines are all close to 1 ($P < 0.005$), demonstrated that the mass signal intensities of the three substances produced by the PI-TOF-MS system could effectively be used to quantify their yields.

With the established quantification lines above, the signal intensities from the close-ended HTP (Fig. 3) were transferred into the aerosol masses, as presented in Fig. 6. When the puff duration was prolonged from 2 to 4 s, the total amount of nicotine could be lowered for 43 % (0.54 to 0.31 mg) under the close-ended airflow configuration. When the puff duration was further increased, the lowest nicotine delivery was 0.05 mg. As the linear regressions ($R^2 > 0.9$) were made between puff durations and PG, VG, Nic masses for the close-ended HTP, this method could be used to predict other aerosol chemical deliveries too.

### 3.4. *Online delivery patterns of PG, VG, Nic and implications*

With the established quantification lines, the advantage of the PI-TOF-MS in time resolution could be utilized to quantify the chemical

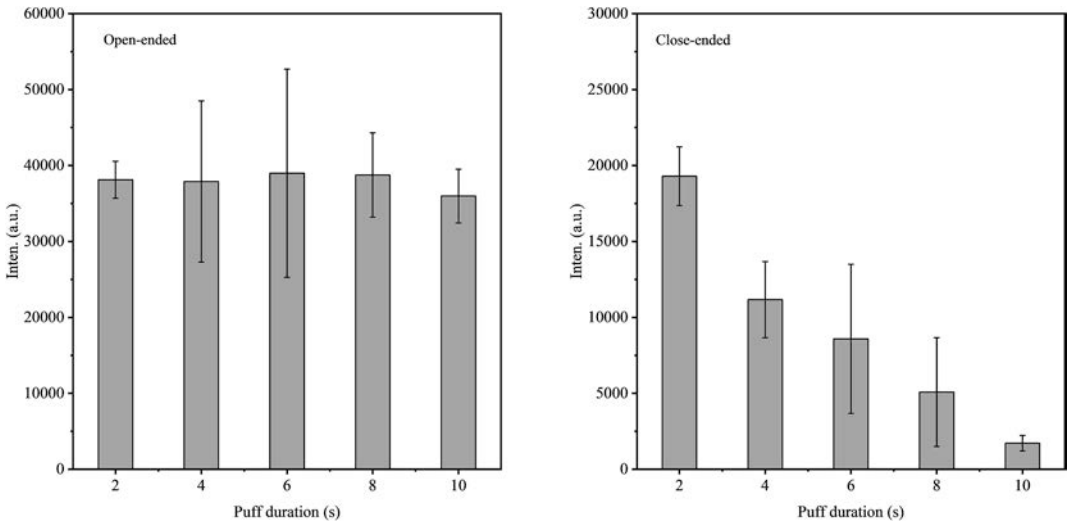


**Fig. 3.** Signals of *m/z* 162 (nicotine) under different puff durations for the open-ended and close-ended products.

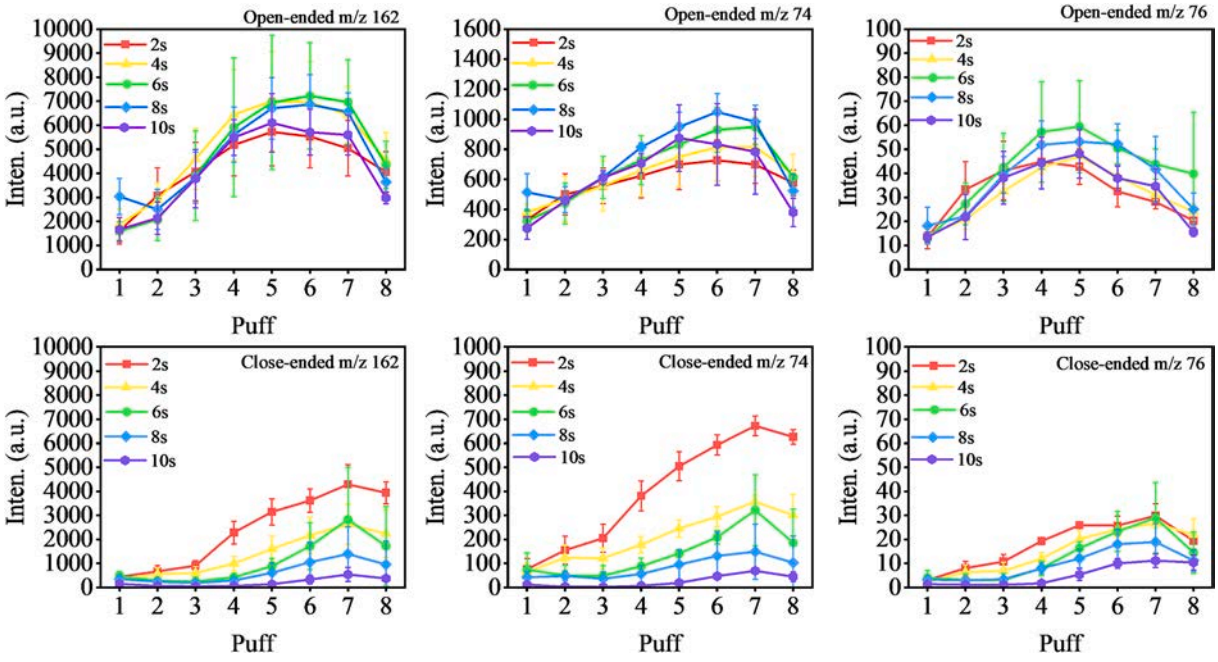


**Fig. 4.** Puff-by-puff release signals of *m/z* 162 (nicotine), *m/z* 74 (glycerin) and *m/z* 76 (propylene glycol) for the open- and close-ended HTPs with different puff durations.

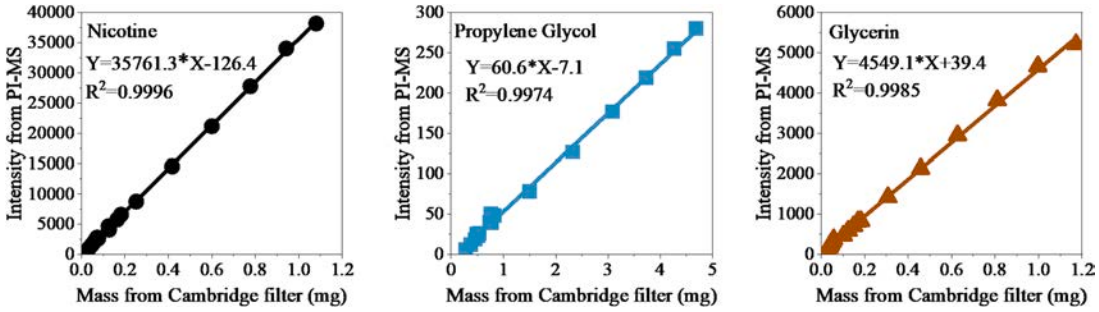


**Fig. 5.** Linear regression between the mass (mg) collected by Cambridge filter and the mass signal intensity of nicotine (*m/z* 162), propylene glycol (*m/z* 76) and glycerin (*m/z* 74) recorded by PI-TOF-MS.

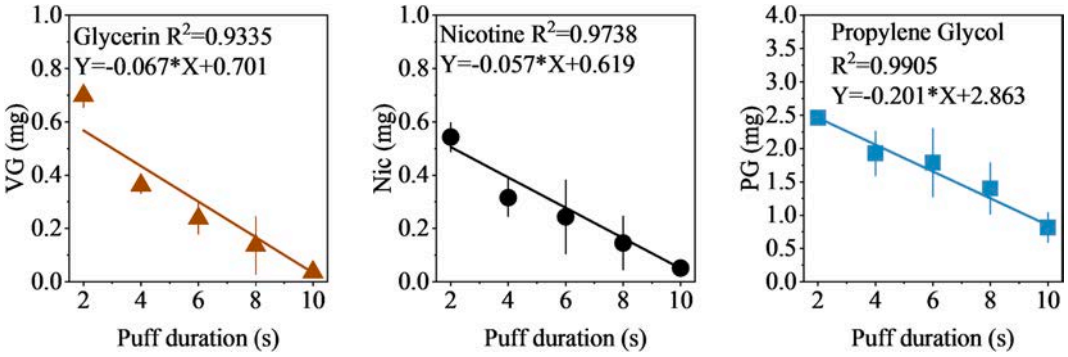


**Fig. 6.** Linear regression between VG, Nic, PG aerosol mass (mg, sum of puff 1–8) and puff durations for the close-ended HTP. Puff volume = 55 mL.

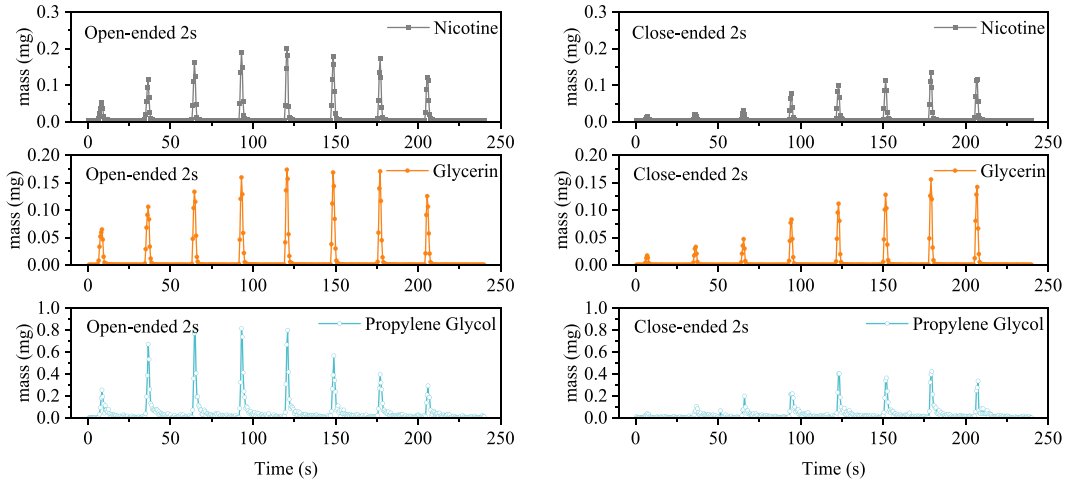


**Fig. 7.** Online aerosol emission profiles for nicotine, glycerin and propylene glycol mass under HCI puffing mode for the open-ended and close-ended HTPs.

delivery in particulate phase within one puff, and some examples were shown in Fig. 7. Generally, similar time-mass profiles were observed between the open-ended and close-ended HTPs. The delivery profiles were approximately bell-shaped, where areas also follow an increase–decrease trend from puffs 1 to 8 as in the puff-by-puff results of Fig. 4. In addition, with the increase of puff durations, both the close-ended and open-ended HTPs exhibited lower but broader curves (Fig S5). For the open-ended HTP, peak areas remained relatively stable, implied that the masses of VG, PG, Nic were similar among the different puff durations. It could be inferred that prolonged puff durations in the open-ended HTP lowered the time release rate while having no effect on volume release rate of the aerosol. On the contrary, increased puff durations induced less peak areas thus lower amount of VG, PG, Nic mass per puff yield from the close-ended HTP, decreased both the time release rate and volume release rate of its aerosol.

Prolonged puff durations under the same puff volume would decrease the flow velocity, and thus would lead to higher probability of particle deposition in the human respiratory tract [36]. Knowing the mass releasing rate of chemicals under different flow velocities, is of great significance to understand their deposition process in human body during smoking, especially for HTPs with a higher deposition fraction to combustion cigarettes [37]. The nicotine releasing rates were obtained in the puff-by-puff experiment and plotted in Fig. 8, as well as the enlarged view of the mass-time profile within the 2 s puff time. The puff-

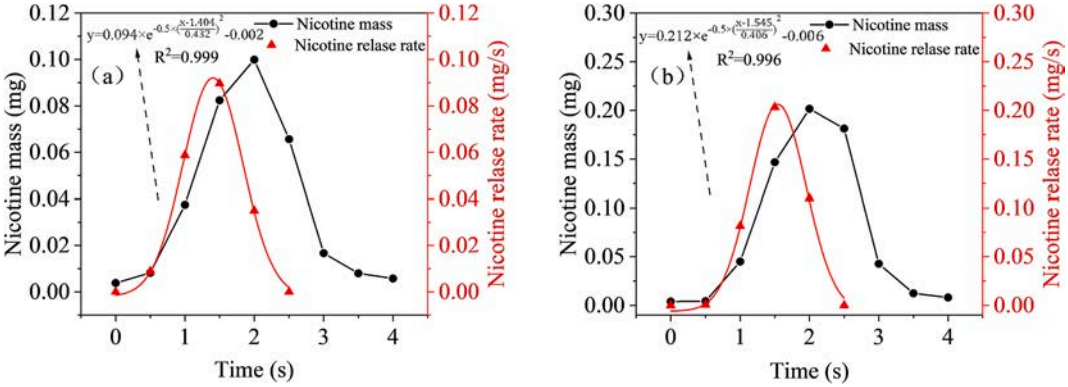


**Fig. 8.** The time-resolved mass profile for nicotine during the puff 5 for the close (a) - and open-ended (b) HTPs. The puff lasted 2 s duration (black line). Gauss fitting of nicotine release rates during the puff.

resolved nicotine showed an increasing trend during the single puff, and then dropped to the background level quickly but lasted for slightly longer than 2 s, similar to the release behavior of volatile substances during a single-puff of a cigarette reported by Mitschke et al. [38]. Contrary to the released mass, the nicotine releasing rate showed an approximate normal distribution pattern in both the close-ended and open-ended HTPs, agreeing well with the bell-shaped airflow pattern. Using Gauss fitting, nicotine release rates of the close-ended and open-ended HTPs at the 2 s puff duration were presented as an example in Fig. 8 too. Nicotine releasing rate kept increasing from 0 to 1.5 s for both two products and then decreased to near the background level rapidly. Despite the similarity in their nicotine releasing patterns, lower peak and average values were observed for the close-ended HTP, indicating that the close-ended HTP delivered less nicotine at equal flow rate. These results emphasized the important role of the downstream ventilation holes (their levels and positions) in the nicotine delivery for the close-ended air pathway.

## 4. Conclusions

The present study used an on-line in-situ approach for the aerosol chemical qualification and quantification, providing mechanistic insights into gaseous/particulate partitioning during the aerosol formation of two heated tobacco products (HTPs). Chemical quantifications by the photoionization time-of-flight mass spectrometry for the key aerosol substances were achieved by using internal standard curves and validated with off-line signal intensities. For the on-line measurements, a time resolution of 0.5 s was achieved. Time-mass profiles were obtained within a single puff for the key aerosol components. The novel method helped to study the aerosol generation and extraction mechanisms in two types of HTPs with close-ended and open-ended airflow configurations. Initial pyrolysis products and intermediates in the gas phase were observed in HTPs aerosol as those in cigarettes smoke, indicating that some thermal breakdown reactions still occurred in HTPs. Changes in puff durations altered aerosol formation and delivery significantly for the HTPs, in particular for the close-ended HTP as compared to the open-ended one, thus providing a way to balance the airflow in order to deliver nicotine.

## CRediT authorship contribution statement

**Yue Zhang:** Writing – original draft, Funding acquisition, Conceptualization. **Shaoxin Ye:** Methodology, Data curation. **Zuoying Wen:** Methodology, Investigation. **Lili Fu:** Writing – review & editing, Resources, Conceptualization. **Tao Wang:** Investigation. **Ke Zhang:** Writing – review & editing, Resources, Conceptualization. **Chuan Liu:** Writing – review & editing. **Shuang Wang:** Methodology, Funding acquisition. **Xiaofeng Tang:** Writing – review & editing, Methodology, Investigation. **Di Kang:** Investigation. **Bing Wang:** Supervision, Resources. **Bin Li:** Supervision, Resources.

## Declaration of competing interest

The authors declare that they have no known competing financial interests or personal relationships that could have appeared to influence the work reported in this paper.

## Data availability

Data will be made available on request.

## Acknowledgement

This research was supported by the National Natural Science Foundation of China (No. 42307152), Innovation projects of Zhengzhou tobacco research institute (No. 252020CR0280), Natural Science Foundation of Henan (No. 222300420389).

## Appendix A. Supplementary data

Supplementary data to this article can be found online at https://doi.org/10.1016/j.microc.2024.110093.

## References

[1] T. Adam, S. Mitschke, T. Streibel, R.R. Baker, R. Zimmermann, Puff-by-puff resolved characterisation of cigarette mainstream smoke by single photon ionisation (SPI)-time-of-flight mass spectrometry (TOFMS): comparison of the 2R4F research cigarette and pure Burley, Virginia, Oriental and Maryland tobacco cigarettes, Anal. Chim. Acta. 572 (2) (2006) 219–229.
[2] X. Wang, Q. Jiang, H. Li, D.D. Chen, Rapid determination of chemical composition in the particulate matter of cigarette mainstream smoke, Talanta. 217 (2020) 121060.
[3] S.G. Carmella, X. Ming, N. Olvera, C. Brookmeyer, A. Yoder, S.S. Hecht, High throughput liquid and gas chromatography–tandem mass spectrometry assays for tobacco-specific nitrosamine and polycyclic aromatic hydrocarbon metabolites associated with lung cancer in smokers, Chem. Res. Toxicol. 26 (8) (2013) 1209–1217.
[4] B. Gao, X. Du, X. Wang, J. Tang, X. Ding, Y. Zhang, X. Bi, G. Zhang, Parent, alkylated, and sulfur/oxygen-containing polycyclic aromatic hydrocarbons in mainstream smoke from 13 brands of Chinese cigarettes, Environ. Sci. Technol. 49 (15) (2015) 9012–9019.
[5] S.H. Edwards, L.M. Rossiter, K.M. Taylor, M.R. Holman, L. Zhang, Y.S. Ding, C. H. Watson, Tobacco-specific nitrosamines in the tobacco and mainstream smoke of US commercial cigarettes, Chem. Res. Toxicol. 30 (2) (2017) 540–551.
[6] N. Mallock, E. Pieper, C. Hutzler, F. Henkler-Stephani, A. Luch, Heated tobacco products: a review of current knowledge and initial assessments, Front. Public. Health. 7 (2019) 287.
[7] B. Li, Y. Sun, L. Fu, L. Feng, P. Lei, C. Liu, J. Han, S. Shang, S. Wang, L. Wang, Aerosol formation and transfer in open-and closed-ended heated tobacco products, Beitr. Tabakforsch. Int. 31 (3) (2022) 162–174.
[8] M.S. Werley, S.A. Freelin, S.E. Wrenn, B. Gerstenberg, E. Roemer, H. Schramke, E. Van Miert, P. Vanscheeuwijck, S. Weber, C.R. Coggins, Smoke chemistry, in vitro and in vivo toxicology evaluations of the electrically heated cigarette smoking system series K, Regul. Toxicol. Pharm. 52 (2) (2008) 122–139.
[9] D.-H. Lim, Y.-H. Kim, Y.-S. Son, S.-H. Jo, K.-H. Kim, A simple sampling method for quantification of hazardous volatile organic compounds in mainstream cigarette smoke: method development and prestudy validation, Microchem. J. 180 (2022) 107602.
[10] X. Li, Y. Luo, X. Jiang, H. Zhang, F. Zhu, S. Hu, H. Hou, Q. Hu, Y. Pang, Chemical analysis and simulated pyrolysis of tobacco heating system 2.2 compared to conventional cigarettes, Nicotine. Tob. Res. 21 (1) (2019) 111–118.
[11] R. Yadav, K. Saoud, F. Rasouli, M. Hajaligol, R. Fenner, Study of cigarette smoke aerosol using time of flight mass spectrometry, J. Anal. Appl. Pyrol. 72 (1) (2004) 17–25.
[12] Y. Pan, Y. Hu, J. Wang, L. Ye, C. Liu, Z. Zhu, Online characterization of isomeric/isobaric components in the gas phase of mainstream cigarette smoke by tunable synchrotron radiation vacuum ultraviolet photoionization time-of-flight mass spectrometry and photoionization efficiency curve simulation, Anal. Chem. 85 (24) (2013) 11993–12001.
[13] T.G. Schwanz, M.G. Nespeca, J.C. Dias, L.V.V. Bokowski, M.C.A. Marcelo, D. H. Maximiano, L.S. Canova, P.B. de Souza Cruz, O.F.S. Pontes, S. Kaiser, GC× GC-TOFMS and chemometrics approach for comparative study of volatile compound release by tobacco heating system as a function of temperature, Microchem. J. 159 (2020) 105578.
[14] B. Savareear, J. Escobar-Arnanz, M. Brokl, M.J. Saxton, C. Wright, C. Liu, J.-F. Focant, Comprehensive comparative compositional study of the vapour phase of cigarette mainstream tobacco smoke and tobacco heating product aerosol, J. Chromatogr. a. 1581 (2018) 105–115.
[15] R. Salman, S. Talih, R. El-Hage, C. Haddad, N. Karaoghlanian, A. El-Hellani, N. Saliba, A. Shihadeh, Free-base and total nicotine, reactive oxygen species, and carbonyl emissions from IQOS, a heated tobacco product, Nicotine. Tob. Res. 21 (9) (2019) 1285–1288.
[16] R. Dusautoir, G. Zarcone, M. Verriele, G. Garçon, I. Fronval, N. Beauval, D. Allorge, V. Riffault, N. Locoge, J. Loguidice, S. Anthérieu, Comparison of the chemical composition of aerosols from heated tobacco products, electronic cigarettes and tobacco cigarettes and their toxic impacts on the human bronchial epithelial BEAS-2B cells, J. Hazard. Mater. 401 (2021) 123417.
[17] L. Cancelada, M. Sleiman, X. Tang, M. Russell, V. Montesinos, M. Litter, L. Gundel, H. Destaillats, Heated tobacco products: volatile emissions and their predicted impact on indoor air quality, Environ. Sci. Technol. 53 (13) (2019) 7866–7876.
[18] S. Mitschke, T. Adam, T. Streibel, R.R. Baker, R. Zimmermann, Application of time-of-flight mass spectrometry with laser-based photoionization methods for time-resolved on-line analysis of mainstream cigarette smoke, Anal. Chem. 77 (8) (2005) 2288–2296.
[19] S. Boué, D. Goedertier, J. Hoeng, A. Kuczaj, S. Majeed, C. Mathis, A. May, B. Phillips, M.C. Peitsch, F. Radtke, State-of-the-art methods and devices for the generation, exposure, and collection of aerosols from heat-not-burn tobacco products, Tox. Res. Appl. 4 (2020) 2397847319897869.

[20] F. Mühlberger, R. Zimmermann, A. Kettrup, A mobile mass spectrometer for comprehensive on-line analysis of trace and bulk components of complex gas mixtures: parallel application of the laser-based ionization methods VUV single-photon ionization, resonant multiphoton ioniza-tion, and laser-induced electron impact ionization, Anal. Chem. 73 (15) (2001) 3590–3604.
[21] T. Streibel, R. Zimmermann, Resonance-enhanced multiphoton ionization mass spectrometry (REMPI-MS): applications for process analysis, Annual Review of Anal. Chem. 7 (2014) 361–381.
[22] H. Cui, S. Ehlert, F. Xie, J. Heide, N. Deng, B. Li, C. Liu, K. McAdam, A. Walte, R. Zimmermann, Integration of time and spatially resolved in-situ temperature and pressure measurements with soft ionisation mass spectrometry inside a burning superslim cigarette, J. Anal. Appl. Pyrol. 135 (2018) 310–318.
[23] J. Hawke, G. Errington, M.B. von Frowein, Evaluation of an online, real-time, soft-photon ionisation time-of-flight mass spectrometer for mainstream tobacco smoke analysis, BMC. Chem. 13 (1) (2019) 1–17.
[24] J. Heide, T.W. Adam, E. Jacobs, J.-M. Wolter, S. Ehlert, A. Walte, R. Zimmermann, Puff-resolved analysis and selected quantification of chemicals in the gas phase of E-cigarettes, heat-not-burn devices, and conventional cigarettes using Single-Photon Ionization Time-of-Flight Mass Spectrometry (SPI-TOFMS): a comparative study, Nicotine. Tob. Res. 23 (12) (2021) 2135–2144.
[25] Y. Hu, C. Liu, Y. Xu, J. Yang, Y. Pan, Identification of isobars and isomers in cigarette sidestream smoke in real time by synchrotron radiation photoionization mass spectrometry and multiple linear regression, Anal. Chem. 93 (14) (2021) 5718–5726.
[26] Z. Wen, X. Gu, X. Tang, X. Li, Y. Pang, Q. Hu, J. Wang, L. Zhang, Y. Liu, W. Zhang, Time-resolved online analysis of the gas-and particulate-phase of cigarette smoke generated by a heated tobacco product using vacuum ultraviolet photoionization mass spectrometry, Talanta. 238 (2022) 123062.
[27] K. Shengye, W. Guanghe, Y. Xueyan, Simultaneous determination of moisture, 1, 2-propylene glycol, nicotine and glycerol in tobacco material for heat-not-burn products by GC-TCD, Tob. Sci. Technol. 53 (5) (2020) 41–46, in Chinese.
[28] D. Zhang, Y. Cao, P. Zhang, J. Liang, K. Xue, Y. Xia, Z. Qi, Investigation of the thermal decomposition mechanism of glycerol: the combination of a theoretical study based on the Minnesota functional and experimental support, Phys. Chem. Chem. Phys. 23 (36) (2021) 20466–20477.
[29] C. AlGemayel, E. Honein, A. El Hellani, R. Salman, N.A. Saliba, A. Shihadeh, J. Zeaiter, Kinetic modeling of the pyrolysis of propylene glycol, Engineered, Science 20 (2022) 162–179.
[30] S. Moldoveanu, W. Coleman, J. Wilkins, Determination of carbonyl compounds in exhaled cigarette smoke, Beitr. Tabakforsch. Int. 22 (5) (2007) 346–357.
[31] H.D. Hoberman, R.C.S. George, Reaction of tobacco smoke aldehydes with human hemoglobin, J. Biochem. Toxic. 3 (2) (1988) 105–119.
[32] M.M. Diallo, S. Laforge, Y. Pouilloux, J. Mijoin, Influence of the preparation procedure and crystallite size of Fe-MFI zeolites in the oxidehydration of glycerol to acrolein and acrylic acid, Catal. Commun. 126 (2019) 21–25.
[33] M.D. McGraw, S.-Y. Kim, C. Reed, E. Hernady, I. Rahman, T.J. Mariani, J. N. Finkelstein, Airway basal cell injury after acute diacetyl (2, 3-butanedione) vapor exposure, Toxicol. Lett. 325 (2020) 25–33.
[34] S. Huang, D. Liu, M. Chen, G. Xi, P. Yang, C. Jia, D. Mao, Effects of Bacillus subtilis subsp. on the microbial community and aroma components of flue-cured tobacco leaves based on metagenome analysis, Arch. Microbiol. 204 (12) (2022) 726.
[35] Z. Guo, S. Wang, K. Zhang, P. Lei, L. Fu, Q. Zhang, S. Shang, S. Wang, L. Wang, M. Zhang, Thermal de-oxygenation to form condensable aerosol from reconstituted tobacco without auto-ignition, Beitr. Tabakforsch. Int. 31 (3) (2022) 130–141.
[36] L. Koblinger, W. Hofmann, Monte Carlo modeling of aerosol deposition in human lungs. Part I: simulation of particle transport in a stochastic lung structure, J. Aerosol. Sci. 21 (5) (1990) 661–674.
[37] Y. Li, H. Cui, L. Chen, M. Fan, J. Cai, J. Guo, C.U. Yurteri, X. Si, S. Liu, F. Xie, Modeled respiratory tract deposition of smoke aerosol from conventional cigarettes, electronic cigarettes and heat-not-burn products, Aerosol. Air. Qual. Res. 21 (5) (2021) 200241.
[38] T. Ferge, J. Maguhn, K. Hafner, F. Mühlberger, M. Davidovic, R. Warnecke, R. Zimmermann, On-line analysis of gas-phase composition in the combustion chamber and particle emission characteristics during combustion of wood and waste in a small batch reactor, Environ. Sci. Technol. 39 (6) (2005) 1393–1402.
[39] R. Hertz-Schünemann, S. Ehlert, T. Streibel, C. Liu, K. McAdam, R. Baker, R. Zimmermann, High-resolution time and spatial imaging of tobacco and its pyrolysis products during a cigarette puff by microprobe sampling photoionisation mass spectrometry, Anal. Bioanal. Chem. 407 (2015) 2293–2299.
[40] C. Busch, T. Streibel, C. Liu, K.G. McAdam, R. Zimmermann, Pyrolysis and combustion of tobacco in a cigarette smoking simulator under air and nitrogen atmosphere, Anal. Bioanal. Chem. 403 (2012) 419–430.
[41] NIST Chemistry WebBook, SRD 69. National Institute of Standards and Technology.https://webbook.nist.gov/cgi/cbook.cgi?Name=Triethyl+citrate&Units=SI&cMS=on.